

Westcott g Factors Extended to Arbitrary Neutron Energy Spectra

D.A. Matters^{a,*}, A.M. Hurst^b and T. Kawano^c

^a*Nuclear Science Division, Lawrence Berkeley National Laboratory, Berkeley, California 94720, USA*

^b*Department of Nuclear Engineering, University of California at Berkeley, Berkeley, California 94720, USA*

^c*Theoretical Division, Los Alamos National Laboratory, Los Alamos, New Mexico 87545, USA*

ARTICLE INFO

Keywords:

Neutron activation analysis
Neutron-capture reactions
Evaluated nuclear data libraries
Westcott g factors

ABSTRACT

Westcott g factors are used in Neutron Activation Analysis (NAA) and Prompt Gamma-ray Activation Analysis (PGAA) to evaluate the impact of non- $1/v$ behavior in the neutron-capture cross sections of certain nuclei on activation product yields. This non- $1/v$ behavior arises from the presence of neutron resonances in the neutron-capture cross sections that overlap with the source neutron spectrum at low (< 5 eV) energies. Historically, Westcott g factors that have been cataloged for NAA and PGAA applications are the result of calculations that assume a Maxwellian neutron velocity distribution with a given average temperature. In this study, we use this approach with updated neutron-capture cross sections from the Evaluated Nuclear Data File, version VIII.1 (ENDF/B-VIII.1) to tabulate Westcott g factor values for a broad range of Maxwellian distribution temperatures, comparing the results against currently-available g factors from International Atomic Energy Agency tables and other sources. It was discovered during this analysis that the use of guided thermal and cold-neutron beams at certain facilities necessitates an approach for evaluating Westcott g factors based on arbitrary non-Maxwellian spectra. In this paper, we present an approach for calculating g factors with user-specified neutron spectra, and we apply these methods to obtain Westcott g -factors for guided- and cold-neutron beams at the Budapest Research Reactor and the Forschungsreaktor München II reactor. Open-source software has been developed as part of this study that can be used to perform these calculations for applications in PGAA and NAA experiments.

1. Introduction

Below approximately 5 eV, the neutron-capture cross sections for most nuclei are inversely proportional to the velocity of the incident neutron. This relationship is sometimes known as the $1/v$ law, although there are a number of notable exceptions to this behavior, known as non- $1/v$ absorbers or irregular nuclei [1, 2, 3]. These irregular nuclei have neutron-capture resonances that overlap the thermal-energy range, which distorts the usual $1/v$ behavior of the capture cross section at thermal and lower velocities.

Thermal-neutron capture cross sections σ_0 are tabulated in sources such as the *Atlas of Neutron Resonances* [2], IAEA tables of pile oscillator results [4], the IRDFF-II neutron metrology library [5], and the Evaluated Gamma-ray Activation File (EGAF) [6]. The recently-developed pyEGAF software package [7, 8] allows users to access, manipulate, and analyze neutron-capture γ -ray data in EGAF database, including querying the database for σ_0 values.

The application of these cross sections in Neutron Activation Analysis (NAA) and Prompt Gamma-Ray Activation Analysis (PGAA) involving irregular nuclei can require adjustment based on the neutron energy spectrum used in experiments. For example, PGAA and NAA experiments are commonly performed at facilities that incorporate research reactors with guided neutron beamlines, such as the Budapest Research Reactor (BRR) and the Forschungsreaktor München II (FRM II) reactor.

To account for the non- $1/v$ behavior of irregular nuclei in a simple way for application in NAA or PGAA, a correction factor known as the Westcott g factor was devised [9, 10]. Using the convention where g_w is the Westcott g factor, starting with a table of neutron-capture cross sections σ_0 for thermal ($v_0 = 2200$ m/s, $E_0 = 0.025$ eV, or $\lambda_0 = 1.8$ Å) neutrons, the cross section (σ) as a function of the neutron velocity v , energy E , or wavelength λ below

*Corresponding author

 damatters@lbl.gov (D.A. Matters)

 <https://github.com/DMatters> (D.A. Matters)

ORCID(s): 0000-0003-4288-2817 (D.A. Matters)

the epithermal region is given by the respective equations

$$\sigma(v) = \sigma_0 g_w \frac{v_0}{v}, \quad (1)$$

$$\sigma(E) = \sigma_0 g_w \sqrt{\frac{E_0}{E}}, \quad (2)$$

or

$$\sigma(\lambda) = \sigma_0 g_w \sqrt{\frac{\lambda}{\lambda_0}}. \quad (3)$$

For a regular nuclide that follows the so-called $1/v$ law, $g_w = 1$ at low neutron velocities. Westcott originally evaluated g factors assuming a Maxwellian neutron energy spectrum with an average temperature T [9], although this can be extended to arbitrary neutron spectra using the methodology described in this paper.

In the sections that follow, we present two alternative methods for calculating Westcott g factors, extending these methods to from Maxwellian distributions to arbitrary neutron spectra, such as those measured experimentally at PGAA and NAA facilities. These methods are implemented in open-source software tools that can be employed by users to calculate g factors for any target nucleus with available neutron-capture cross section data. Results from using these software tools are then compared to show the advantages of using cross sections from evaluated libraries and experimental neutron energy spectra instead of approximations to calculate Westcott g factors.

2. Calculating Westcott g Factors

In general, the g factor is given in terms of the neutron density distribution function $p_T(v)$ by the expression

$$g_w(T) = \frac{\int_0^\infty \sigma(v) \cdot v \cdot p_T(v) dv}{\sigma_0 v_0}. \quad (4)$$

Evaluating this integral directly can be difficult, depending on the availability of cross section data $\sigma(v)$ at various neutron velocities. Experimental cross-section data are available at discrete energies, and libraries such as the Evaluated Nuclear Data File (ENDF) [11] include modeled cross sections where experimental data are unavailable or insufficient.

2.1. Irregularity Functions

An approximate method for calculating Westcott g factors is outlined in Ref. [3], and involves integrating over low-energy neutron resonances that give rise to the non- $1/v$ behavior in the capture cross section. Neutron resonance data from the *Atlas of Neutron Resonances* [2] are used to define an irregularity function $\delta_0(v)$, which is the Lorentzian part of the Breit-Wigner formula [3, 12]. The irregularity function describes the behavior of the cross section as a function of neutron velocity near a resonance of energy E_r and total width Γ , according to the function

$$\delta_0(v) = \frac{\left(E_r - \frac{1}{2}m_n v_0^2\right)^2 + \Gamma^2/4}{\left(E_r - \frac{1}{2}m_n v^2\right)^2 + \Gamma^2/4}, \quad (5)$$

where m_n is the neutron mass. With the irregularity function defined above, the Westcott g factor can be approximated as

$$g_w(T) \approx \int_0^\infty \delta_0(v) \cdot p_T(v) dv. \quad (6)$$

When there is more than one resonance, the lowest-energy resonance is commonly used to define the function $\delta_0(v)$ in Eq. 5 [3]. However, doing so implicitly assumes that the lowest-energy resonance provides the dominant

contribution to the non- $1/v$ behavior of the neutron-capture cross section. In general, this may not always be true, and the approximation inherent in Eq. 6 may not be valid in cases where there are multiple low-energy resonances or resonances reported with negative energies relative to the neutron-separation energy [2]. In these cases, a more accurate method for calculating Westcott *g* factors is to integrate over the entire neutron-capture cross section as defined in reaction data libraries such as the ENDF.

Resonance parameters, including the total widths Γ and energies E_r , are tabulated in ENDF/B-VIII.1 [11, 13], the *Atlas of Neutron Resonances* [2], and the *Handbook of Prompt Gamma Activation Analysis* [3]. The resonance parameters from these sources were used to evaluate Westcott *g* factors using the irregularity function method outlined above for six representative irregular nuclei: ^{83}Kr , ^{115}In , ^{149}Sm , ^{151}Eu , ^{157}Gd , and ^{176}Lu . These six non- $1/v$ absorbers provide good exemplars for demonstrating the calculation of Westcott *g* factors, with cross sections that range from nearly- $1/v$ behavior (e.g., ^{83}Kr) to highly irregular (e.g., ^{157}Gd), involving a range of resonance energies and widths, as listed in Table 1.

Table 1

Neutron-capture cross section resonance energies E_r and total widths Γ for select non- $1/v$ nuclei, for low-energy resonances with $E_r < 5$ eV, from ENDF/B-VIII.1 [11, 13], the *Handbook of Prompt Gamma Activation Analysis* (PGAA Handbook [3]), and the *Atlas of Neutron Resonances* [2]. Bold text indicates the parameters used to calculate Westcott *g* factors via the irregularity function method in this study.

| Isotope | ENDF/B-VIII.1 ^a | | <i>Atlas of Neutron Resonances</i> | | PGAA Handbook | |
|-------------------|----------------------------|--------------------------|------------------------------------|----------------|----------------------|-------------------|
| | E_r (eV) | Γ (meV) | E_r (eV) | Γ (meV) | E_r (eV) | Γ (meV) |
| ^{83}Kr | -9.81 | 384 | -9.81 | 252 | -3.9 | 245 |
| ^{115}In | 1.457 | 75.0 | 1.457 | 72 | 1.457 | 75.04 |
| | 3.85 | 81.4 | 3.85 | 81 | 3.86 | 81.2 |
| ^{149}Sm | -1.127 | 71.9 | -1.127 | 64.9 | -1.5 | 87.4 |
| | 0.0973 | 63.4 | 0.0973 | 62.9 | 0.0973 | 61 |
| | 0.872 | 61.5 | 0.872 | 60.8 | 0.872 | 60.5 |
| | 4.94 | 65.9 | 4.94 | 64 | 4.95 | 63.1 |
| ^{151}Eu | -0.0609 | 105.3 | -0.00362 | 95.8 | 0.00361 ^b | 95.8 |
| | 0.321 | 79.6 | 0.327 | 79.5 | 0.321 | 79.6 |
| | 0.46 | 87.7 | 0.465 | 87 | 0.461 | 87.7 |
| | 1.055 | 88.2 | 1.054 | 85.7 | 1.055 | 85.2 |
| | 1.815 | 91.0 | 1.806 | 95 | 1.83 | 90 |
| | 2.717 | 94.2 | 2.717 | 92 | 2.717 | 93.2 |
| | 3.368 | 95.2 | 3.370 | 88 | 3.366 | 95.2 |
| | 3.71 | 93.9 | 3.711 | 92 | 3.71 | 94 |
| | 4.79 | 91.2 | 4.796 | 66 | 4.78 | 90 |
| ^{157}Gd | 0.0314 | 107.7^c | 0.0314 | 107 | 0.0314 | 106 |
| | 2.825 | 97.3 | 2.827 | 98 | 2.83 | 97 |
| ^{176}Lu | 0.1413 | 62.4 | 0.1379 | 65.0 | 0.141 | 62.4 |
| | 1.565 | 59.5 | 1.569 | 59 | 1.565 | 59.5 |
| | 4.36 | 68.4 | 4.316 | 65 | 4.36 ^d | 68.4 ^d |

^aResonance parameters were taken from the Breit-Wigner tables, except where otherwise noted.

^bA negative sign, omitted in Ref. [3], is present in ENDF/B-VI.8 (the source for parameters in the PGAA Handbook).

^cThe total resonance width is equal to the sum of the Reich-Moore resonance widths listed in ENDF/B-VIII.1.

^dResonance parameters evidently used to calculate the ^{176}Lu *g*-factors in the PGAA Handbook; see Table 3.

2.2. Cross Sections from ENDF/B-VIII.1

While irregularity functions provide a straightforward method for calculating Westcott *g* factors from readily-available neutron-capture resonance widths such as those in Ref. [2], the method can produce errors for nuclei that have multiple low-energy resonances. To illustrate the effect of low-energy resonances, neutron-capture cross sections for each of the nuclei listed in Table 1 are shown in Fig. 1.

It is evident from Fig. 1(b-f) that for a number of irregular nuclei, the capture cross section below 5 eV cannot be approximated simply with a single Lorentzian lineshape. A more appropriate method that can be applied generally to

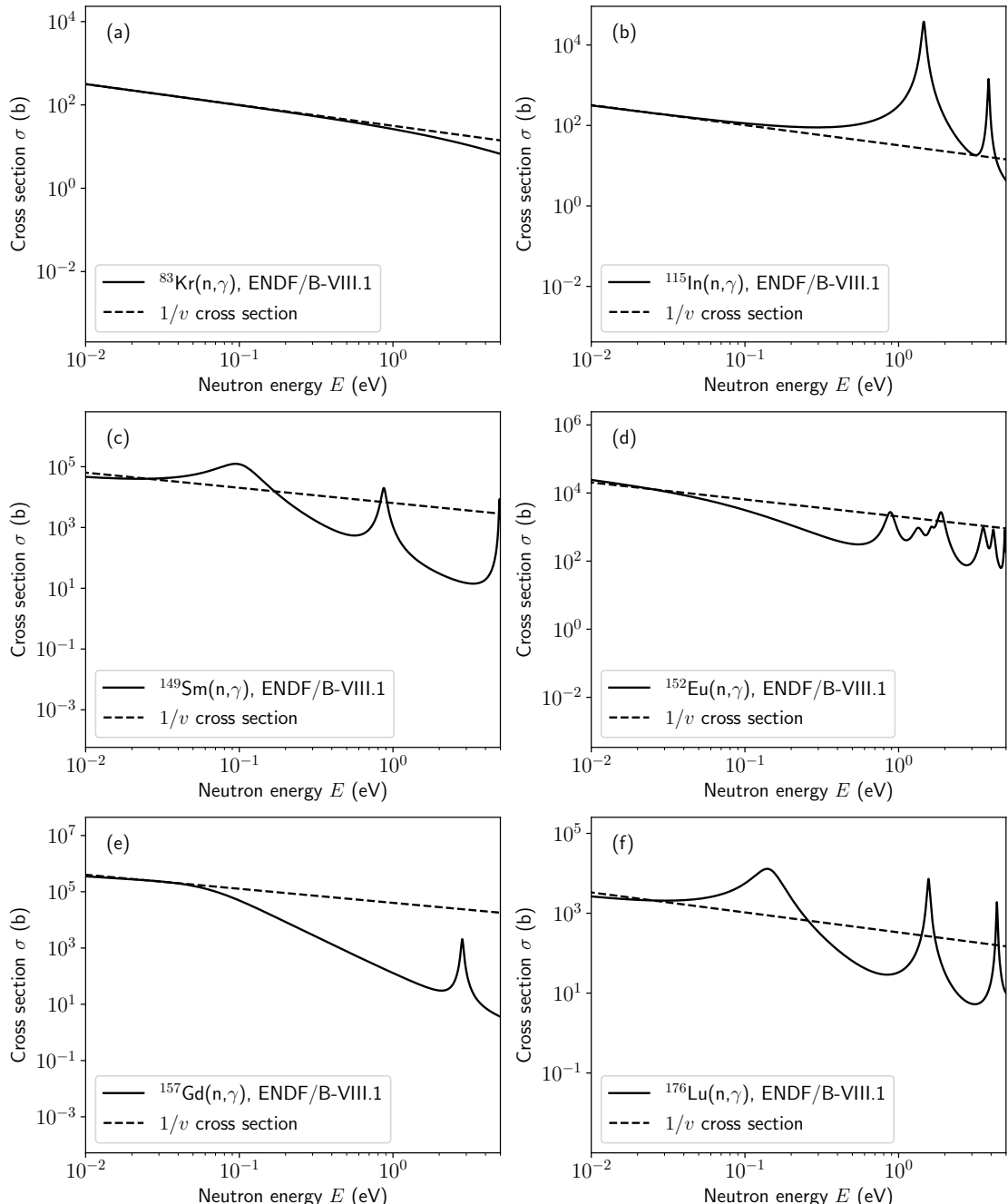


Figure 1: Low-energy ($E \leq 5$ eV) neutron-capture cross sections from ENDF/B-VIII.1 [13] for each of the isotopes listed in Table 1. The ENDF/B-VIII.1 cross sections (σ) are plotted against hypothetical linear (on the log-scale plot) $1/v$ cross sections to show the irregular behavior of these nuclei due to the presence of capture resonances.

evaluate g_w is to use the full neutron-capture cross section defined in evaluated nuclear data libraries such as ENDF/B-VIII.1 and numerically integrate Eq. 4 directly. To do this requires defining the cross section $\sigma(v)$ at all neutron velocities v .

In practice, this was done in two different ways. First, the DeCE (Descriptive Correction of ENDF-6 format) tool [14, 15], a C++ code that interfaces with cross sections in the ENDF-6 format, was modified to calculate Westcott g

factors by numerically integrating Eq. 4. Second, a purpose-built tool called `WestcottFactors` was written in Python to ingest ENDF cross sections in the Generalized Nuclear Database Structure (GNDS) format [16] and perform the integration. Both the `DeCE` and `WestcottFactors` codes were then modified with the functionality to ingest CSV-formatted experimental neutron-flux distributions, to provide greater functionality to users. These codes are described in further detail below, and results are compared in Sec. 3 to demonstrate consistency between the two methods. The advantage of providing two different tools for calculating Westcott g factors with Maxwellian or user-defined neutron spectra are that users can choose to use either tool based on their comfort with different ENDF formats. Traditional users of ENDF already familiar with the ENDF-6 format may find the `DeCE` method appealing, while early adopters of the GNDS format may elect to use the `WestcottFactors` toolkit. `WestcottFactors` is also a stand-alone tool packaged with cross-section data extracted from ENDF/B-VIII.1 in a publicly-accessible GitHub repository [17] and Python Package Index (PyPI) package [18], and the only requirement for calculating Westcott g factors is a cursory knowledge of Python.

2.2.1. DeCE

The neutron-capture cross section data can be reconstructed from the resonance parameters in ENDF/B-VIII.1, and they are combined with the cross section data in MF (quantity) number 3, MT (reaction type) number 102 in the ENDF-6 formatted file for each nuclide in the library. These combined data are again stored in the MF=3 and MT=102 section for neutron energies ranging from 0.01 meV to 20 MeV. Codes such as `DeCE` [14] can be used to interface with data in the ENDF library using the legacy ENDF-6 plain-text format, and extract or manipulate the data for the purpose of evaluating Westcott g factors. The development branch of `DeCE` [19] was modified to include routines for calculating Westcott g factors for Maxwellian neutron velocity distributions using cross-section data in the ENDF-6 format [20].

2.2.2. WestcottFactors

Starting with the ENDF/B-VIII version of the library, nuclear data were released in Generalized Nuclear Database Structure (GNDS) format [16] alongside the ENDF-6 format. The GNDS format was developed to make nuclear data more accessible through the use of modern computational tools, and it lends itself to interpretation and manipulation by a variety of Python data science packages such as `pandas` [21]. In this work, we developed Python scripts to work with `FUDGE` [22, 23] to extract data from ENDF/B-VIII.1 and interpolate the neutron-capture cross sections stored in MF=3, MT=102. As part of the `WestcottFactors` package, a representative Jupyter notebook is included that provides users with the capability to extract cross sections from GNDS-formatted data, although this is not necessary to use the tool because capture cross-section data from ENDF/B-VIII.1 are already included with the package [17, 18].

Numerical integration methods in the `scipy` package [24] were then used to integrate over the cross sections and neutron density distributions to evaluate Westcott g factors according to Eq. 4. The scripts used to perform these calculations have been packaged into the `WestcottFactors` tool, along with CSV-formatted cross-section data parsed from ENDF/B-VIII.1 and explanatory Jupyter notebooks to demonstrate and interact with the code. The open-source `WestcottFactors` package is available via a publicly-accessible GitHub repository and PyPI package [17, 18]. `WestcottFactors` leverages modern scientific computing libraries to provide a robust method for calculating Westcott g factors in a way that is transparent and traceable end-to-end. It can also be easily modified to ingest data from future versions of the ENDF library as they are released.

2.3. Neutron Velocity Distributions

Several references list Westcott g factors for Maxwellian neutron velocity distributions [1, 3, 25, 26, 27, 28, 29], as do the original papers by Westcott on this topic [9, 10]. Other simplified distributions, such as those for idealized guided-neutron beams, are also included in some references [3].

A Maxwellian velocity distribution is a reasonable simplification for well-moderated neutron sources, and it has the added benefit of being straightforward to integrate in the calculation of Westcott g factors. For a Maxwellian neutron source with temperature T , the normalized neutron density $p_T(v)$ in Eq. 4 is given by

$$p_T(v) = \frac{4}{\sqrt{\pi}} \frac{v^2}{v_T^3} e^{-\frac{v^2}{v_T^2}}, \quad (7)$$

where $v_T = \sqrt{2kT/m_n}$ and k is the Boltzmann constant. The methodology employed for a Maxwellian neutron velocity distribution can be extended to arbitrary neutron spectra through the relationship

$$p_T(v) = \frac{2}{\sqrt{\pi}} \frac{v_T}{v} \phi(v), \quad (8)$$

where $\phi(v)$ is the neutron flux as a function of velocity, normalized such that $\int_0^\infty p_T(v)dv = 1$ [3].

In general, the flux profiles for most neutron sources do not follow pure Maxwellian distributions. In some references, such as [29], this issue is handled by identifying the average temperature for which the Maxwellian distribution most closely matches the actual neutron spectrum, and using the value of g_w for that temperature. In this analysis, spectra from the PGAA beamlines at the BRR and FRM II were used as exemplars for evaluating Westcott *g* factors for arbitrary neutron spectra (excluding epithermal and higher-energy sources). Particularly for the BRR spectra, the spectra were sufficiently different from a Maxwellian shape that the method of matching a Maxwellian distribution to the actual spectra was insufficient to derive an accurate value for g_w to apply with these neutron sources. The BRR and FRM-II neutron spectra are described in further detail below.

2.3.1. BRR

At the BRR, the neutron beamline from the reactor to the PGAA station can be cooled in a liquid H₂ cold cell prior to transiting a nickel supermirror guide, which removes the epithermal component from the neutron spectrum at the target position. In the 30-m distance between the cold cell and the target, neutron temperatures increase to an average energy of 12 meV, corresponding to a temperature of 140 K at the target, as measured by time-of-flight techniques [30, 31]. The neutron density $p_T(v)$ according to the BRR flux profile given by Eq. 8 from such a measurement [31] is shown in Fig. 2, along with that of an older spectrum from the BRR operated without the cold source [32]. Theoretical Maxwellian neutron density functions defined according to Eq. 7 with $T = 140$ K and $T = 293$ K are included in Fig. 2(a) for comparison with the reactor distributions.

2.3.2. FRM II

The neutron energy spectrum from the cold-neutron PGAA beamline at FRM II also employs liquid deuterium cooling and a supermirror guide. The source spectrum has an average neutron energy of 1.8 meV [33], corresponding to a temperature of $T = E/k = 21$ K. Again, a theoretical Maxwellian neutron density defined according to Eq. 7 with $T = 21$ K is included in Fig. 2(b) for comparison with the reactor distribution.

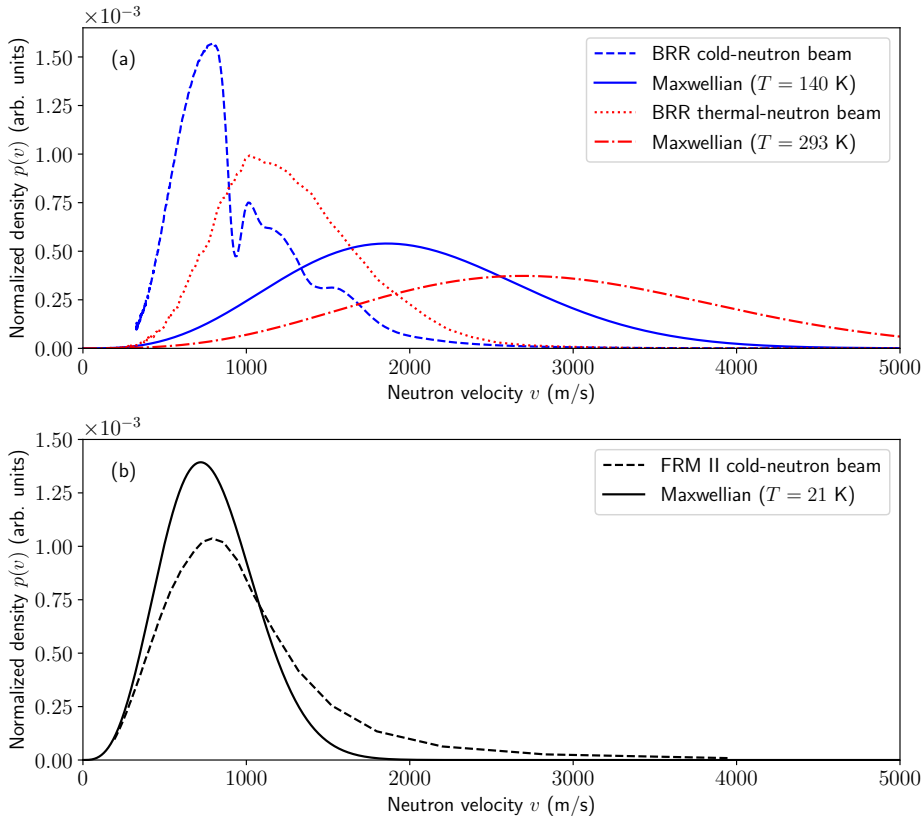


Figure 2: Normalized neutron density functions $p(v)$ for guided cold- and thermal-neutron beams from the PGAA beamlines at the Budapest Research Reactor [30, 31] (a) and the FRM II reactor [33] (b), compared with Maxwellian thermal-neutron density functions $p_T(v)$ at various average temperatures T .

It is evident from Fig. 2(a) that Maxwellian distributions are poor representations of the BRR neutron velocity distributions, particularly if one attempts to use a thermal ($T = 293$ K) Maxwellian distribution to represent the reactor spectrum without the cold source operational. The disagreement between the BRR cold-neutron source spectrum and a Maxwellian distribution with $T = 140$ K is also apparent, even though the measured average beam temperature was 140 K. The velocity distribution of the cold-neutron beam at FRM II PGAA facility more closely resembles a Maxwellian distribution with an average temperature of 21 K, but the Maxwellian is noticeably narrower than the measured distribution in Fig. 2(b). In Sec. 3.3, we will show how these differences in neutron spectra can have a marked impact on the calculated Westcott g factor for non- $1/v$ nuclei.

For DeCE, a fork to the development branch on GitHub [34] was created that incorporates the capability to ingest user-defined, CSV-formatted neutron energy spectra, and uses them to calculate Westcott g factors. This same capability resides natively in the `WestcottFactors` toolkit, and the code is packaged with spectra from BRR and FRM II in the public GitHub repository and PyPI package [17, 18].

3. Results

The methods for calculating Westcott g factors described in Sec. 2 were compared in several steps to identify differences between the methods. The irregular isotopes used for these comparisons were the same as the set of isotopes in Table 1, spanning the space from nearly- $1/v$ to highly irregular behavior in their low-energy neutron-capture cross sections.

3.1. Comparison Between Irregularity Function Method and References

As described in Sec. 2.1, the Westcott g factor calculations in this paper used the lowest-energy resonance (highlighted in bold text in Table 1) for each nucleus to define the irregularity function of Eq. 5. The results of these calculations are shown in Table 2, alongside the published reference Westcott g factors from the IAEA Database [1] and the PGAA Handbook [3] for Maxwellian neutron velocity distributions with various average temperatures T , where available. The columns labeled ‘ENDF’ and ‘Atlas’ in Table 2 list the results from calculating Westcott g factors with the resonance parameters from the respective source highlighted in Table 1.

Table 2

Westcott g factors calculated with the irregularity function method, with parameters from ENDF/B-VIII.1 [11, 13] and the *Atlas of Neutron Resonances* [2] for select non- $1/v$ nuclei, using Maxwellian neutron energy distributions with varying average temperatures T . Included for comparison are the reference Westcott g factor values from the IAEA *Database of Prompt Gamma Rays from Slow Neutron Capture for Elemental Analysis* ([1]) and the PGAA Handbook ([3]).

| Isotope | T (K) | g_w (ENDF [11, 13]) | g_w (Atlas [2]) | g_w (IAEA [1]) | g_w (PGAA [3]) |
|-------------------|---------|-----------------------|-------------------|------------------|--------------------|
| ^{83}Kr | 100 | 1.003 | 1.003 | 1.006 | 1.006 |
| | 200 | 1.000 | 1.000 | 1.000 | 1.000 |
| | 293 | 0.997 | 0.997 | 0.995 | 0.994 |
| | 400 | 0.995 | 0.995 | 0.988 | |
| | 500 | 0.992 | 0.992 | 0.982 | |
| | 600 | 0.990 | 0.990 | 0.976 | |
| ^{115}In | 100 | 0.983 | 0.983 | 0.984 | 0.983 |
| | 200 | 1.001 | 1.001 | 1.002 | 1.002 |
| | 293 | 1.019 | 1.019 | 1.019 | 1.019 |
| | 400 | 1.041 | 1.041 | 1.041 | |
| | 500 | 1.062 | 1.062 | 1.062 | |
| | 600 | 1.085 | 1.085 | 1.084 | |
| ^{149}Sm | 100 | 0.797 | 0.797 | 0.800 | 0.799 |
| | 200 | 1.227 | 1.230 | 1.239 | 1.245 |
| | 293 | 1.694 | 1.702 | 1.718 | 1.738 |
| | 400 | 2.088 | 2.100 | 2.119 | |
| | 500 | 2.290 | 2.305 | 2.325 | |
| | 600 | 2.372 | 2.389 | 2.409 | |
| ^{151}Eu | 100 | 1.266 | 1.201 | 1.161 | 1.128 ^a |
| | 200 | 1.059 | 1.010 | 1.010 | 0.974 ^a |
| | 293 | 0.919 | 0.865 | 0.900 | 0.843 ^a |
| | 400 | 0.798 | 0.736 | 0.811 | |
| | 500 | 0.710 | 0.642 | 0.761 | |
| | 600 | 0.639 | 0.567 | 0.743 | |
| ^{157}Gd | 100 | 0.883 | 0.881 | 0.887 | 0.881 |
| | 200 | 0.898 | 0.897 | 0.899 | 0.896 |
| | 293 | 0.853 | 0.852 | 0.852 | 0.851 |
| | 400 | 0.782 | 0.780 | 0.779 | |
| | 500 | 0.713 | 0.712 | 0.710 | |
| | 600 | 0.651 | 0.649 | 0.647 | |
| ^{176}Lu | 100 | 0.845 | 0.843 | 0.847 | 0.995 ^b |
| | 200 | 1.167 | 1.168 | 1.176 | 1.000 ^b |
| | 293 | 1.714 | 1.699 | 1.752 | 1.003 ^b |
| | 400 | 2.463 | 2.396 | 2.545 | |
| | 500 | 3.080 | 2.953 | 3.205 | |
| | 600 | 3.545 | 3.362 | 3.704 | |

^aValues could only be reproduced using $E_r = +0.00361$ eV; see note in Table 1.

^bValues could only be reproduced using $E_r = 4.36$ eV and $\Gamma = 68.4$ meV; see note in Table 1.

It is evident in Table 2 that the irregularity function method reliably reproduces the published data in Ref. [1] to within 1% in most cases, and that the Westcott g factors are not especially sensitive to the source (ENDF/B-VIII.1 or *Atlas of Neutron Resonances*) of the resonance parameters used. The methodology described in the IAEA Database

involves using the ENDF utility code INTER [35] to generate Westcott g factors by direct integration of the neutron cross sections. Despite using different methods, the two references arrive at similar values of g_w for the same Maxwellian temperatures, except for the highly irregular isotope ^{176}Lu , where differences grow to 4.5% at 600 K between the calculated g factors and those in the IAEA Database.

The irregularity function method described in Sec. 2.1 was used to create the table of Westcott g factors in the PGAA Handbook [3], where the resonance parameters were taken from ENDF/B-VI [36] and are slightly different than those in ENDF/B-VIII.1. By using the resonance parameters in the PGAA Handbook [3] listed in Table 1, we were able to reproduce the g factors listed in that reference using the irregularity function method, with two exceptions. The g factors in the PGAA Handbook differ from the calculated values for ^{151}Eu and ^{176}Lu : for ^{151}Eu , these differences were attributed to a missing sign in the resonance parameters in [3], and for ^{176}Lu it was likely due to the use of a higher-energy resonance to calculate the values in the PGAA Handbook.

3.2. Comparison Between Irregularity Function and Cross-Section Integration Methods

The irregularity function method described in Sec. 2.1 was then compared to the cross-section integration method outlined in Sec. 2.2, by calculating Westcott g factors for the same set of comparator isotopes as in Table 2. The results of these calculations, which were performed using the `WestcottFactors` toolkit developed as part of this study, are shown in Table 3. Here, resonance parameters and cross sections were taken from ENDF/B-VIII.1 [11, 13] for both sets of g -factor calculations. For comparison, the values of g_w from the IAEA *Database of Prompt Gamma Rays from Slow Neutron Capture for Elemental Analysis* ([1]) and the PGAA Handbook ([3]) for Maxwellian neutron spectra with the same temperatures are included.

While the Westcott g factors in Table 3 for some isotopes, such as ^{83}Kr and ^{115}In , show little difference between the irregularity function and cross-section integration methods, these isotopes also have the closest to $1/v$ behavior of the irregular nuclei used in this comparison. This is evident from the fact that their Westcott g factors are within 4% percent of unity for Maxwellian temperatures between 100-600 K.

For other, more irregular nuclei such as ^{149}Sm , ^{151}Eu , ^{157}Gd , and ^{176}Lu , which have Westcott g factors that differ substantially from unity, the method used to calculate g factors can have a large effect. For instance, at Maxwellian temperatures between 200-600 K, the irregularity function method produces Westcott g factors for ^{176}Lu that are approximately 20% lower than those obtained by integrating over the full neutron-capture cross section. These results suggest that the assumption employed in the irregularity function method, where the lowest-energy resonance dominates the capture cross section at low neutron energies, is an oversimplification that is only valid for $1/v$ or near- $1/v$ nuclei. The more accurate method of integrating over the cross sections in the ENDF/B-VIII.1 libraries, which is employed in DeCE and the `WestcottFactors` tool described in this manuscript, should be used for nuclei with multiple low-energy resonances in their neutron-capture cross sections.

3.3. Extension to Arbitrary Non-Maxwellian Neutron Spectra

The `WestcottFactors` toolkit has the advantage of being able to easily ingest reactor neutron energy spectra in a transparent way, so the code [17, 18] incorporates this functionality. We demonstrate it here with the experimental BRR and FRM II spectra described in Sec. 2.3. Westcott g factors were calculated using the ENDF/B-VIII.1 cross sections with the BRR and FRM II neutron density functions shown in Fig. 2. The results are shown in Table 4.

A comparison between the Westcott g factors for the BRR and FRM II neutron sources and Maxwellian spectra with average temperatures that might be used to describe these sources reveals significant differences for ^{151}Eu and ^{157}Gd , suggesting that g_w for non- $1/v$ nuclei depends strongly on the specific neutron spectrum used in activation measurements. Because Maxwellian spectra are idealized and do not generally resemble the neutron spectra used in most thermal- and cold-neutron activation experiments, values for g_w used to adjust thermal-neutron cross sections should be calculated with the measured neutron flux whenever the spectrum is available. The `WestcottFactors` package [17, 18] and the modified DeCE fork [34] provide users with a capability for performing these calculations with any CSV-formatted neutron energy spectrum.

3.4. Comparison Between DeCE and `WestcottFactors`

Next, calculations of Westcott g factors using ENDF/B-VIII.1 cross sections, as described in Sec. 2.2, were carried out using both DeCE and the `WestcottFactors` tool. The results of running the Westcott g factor calculator in the DeCE development branch [19] are listed alongside the corresponding results from running the `WestcottFactors` tool in Table 5 for Maxwellian neutron velocity distributions with various average temperatures T . Additionally, calculations

Table 3

Westcott g factors calculated for select non- $1/v$ nuclei using Maxwellian neutron velocity distributions with average temperatures T between 100-600 K. For the irregularity function method, resonance parameters are from ENDF/B-VIII.1, and for the cross-section integration method, cross sections were taken from GNDS-formatted data in ENDF/B-VIII.1. Percentage differences between the g_w values obtained using the two methods are included to facilitate comparison.

| Isotope | T (K) | g_w (Irregularity Function) | g_w (Cross Section Integration) | % Difference |
|-------------------|---------|-------------------------------|-----------------------------------|--------------|
| ^{83}Kr | 100 | 1.003 | 1.002 | -0.1 |
| | 200 | 1.000 | 0.998 | -0.1 |
| | 293 | 0.997 | 0.995 | -0.2 |
| | 400 | 0.995 | 0.992 | -0.3 |
| | 500 | 0.992 | 0.989 | -0.4 |
| | 600 | 0.990 | 0.985 | -0.4 |
| ^{115}In | 100 | 0.983 | 0.989 | 0.6 |
| | 200 | 1.001 | 1.014 | 1.2 |
| | 293 | 1.019 | 1.038 | 1.8 |
| | 400 | 1.041 | 1.067 | 2.5 |
| | 500 | 1.062 | 1.097 | 3.1 |
| | 600 | 1.085 | 1.128 | 3.8 |
| ^{149}Sm | 100 | 0.797 | 0.893 | 10.7 |
| | 200 | 1.227 | 1.539 | 20.3 |
| | 293 | 1.694 | 2.134 | 20.6 |
| | 400 | 2.088 | 2.503 | 16.6 |
| | 500 | 2.290 | 2.593 | 11.7 |
| | 600 | 2.372 | 2.541 | 6.6 |
| ^{151}Eu | 100 | 1.266 | 1.146 | -10.4 |
| | 200 | 1.059 | 0.954 | -11.0 |
| | 293 | 0.919 | 0.841 | -9.3 |
| | 400 | 0.798 | 0.765 | -4.3 |
| | 500 | 0.710 | 0.741 | 4.2 |
| | 600 | 0.639 | 0.763 | 16.3 |
| ^{157}Gd | 100 | 0.883 | 0.912 | 3.2 |
| | 200 | 0.898 | 0.890 | -0.9 |
| | 293 | 0.853 | 0.802 | -6.3 |
| | 400 | 0.782 | 0.693 | -12.7 |
| | 500 | 0.713 | 0.603 | -18.4 |
| | 600 | 0.651 | 0.526 | -23.7 |
| ^{176}Lu | 100 | 0.845 | 0.911 | 7.2 |
| | 200 | 1.167 | 1.432 | 18.5 |
| | 293 | 1.714 | 2.302 | 25.5 |
| | 400 | 2.463 | 3.330 | 26.0 |
| | 500 | 3.080 | 4.025 | 23.5 |
| | 600 | 3.545 | 4.426 | 19.9 |

using the DeCE development fork that permits users to specify the neutron energy spectrum [34] were compared against similar calculations for the BRR and FRM II spectra using the `WestcottFactors` tool. The non- $1/v$ nuclei used in the comparison are the same as those listed in Table 1.

It is clear from Table 5 that the modified DeCE code and the `WestcottFactors` tool described in this manuscript, which both employ the cross-section integration methodology outlined in Sec. 2.2, produce nearly identical Westcott g factors regardless of the neutron spectra used. Because cross-section data from ENDF/B-VIII.1 were used in both the DeCE and `WestcottFactors` calculations, the small variations of less than 1% in the g factors result from slight differences in the interpolation and numerical integration methods used in the two codes.

3.5. Tabulated Westcott g Factors for Irregular Isotopes With Maxwellian Distributions

The close agreement between the Westcott g factors calculated using the modified DeCE code and the `WestcottFactors` tool provides confidence in the methods used. `WestcottFactors` was then employed to produce a table of $g_w(T)$

Table 4

Comparison of Westcott g factors for select non- $1/v$ nuclei using Maxwellian neutron velocity distributions, BRR cold- and thermal-neutron spectra, and the FRM-II cold-neutron spectrum.

| Isotope | g_w (140 K) | g_w , BRR cold | g_w (293 K) | g_w , BRR thermal | g_w (21 K) | g_w , FRM II cold |
|-------------------|---------------|------------------|---------------|---------------------|--------------|---------------------|
| ^{83}Kr | 1.000 | 1.003 | 0.995 | 0.958 | 1.004 | 1.001 |
| ^{115}In | 0.999 | 0.982 | 1.038 | 2.046 | 0.971 | 0.993 |
| ^{149}Sm | 1.115 | 0.799 | 2.134 | 0.776 | 0.641 | 1.082 |
| ^{151}Eu | 1.058 | 1.237 | 0.841 | 1.150 | 1.385 | 1.135 |
| ^{157}Gd | 0.919 | 0.869 | 0.802 | 0.833 | 0.803 | 0.872 |
| ^{176}Lu | 1.063 | 0.848 | 2.302 | 0.917 | 0.728 | 1.013 |

values similar to that in the IAEA database [1], which is included in the Appendix as Table A1. The set of mostly-irregular isotopes includes those from the IAEA database, as well as those from Refs. [3, 26, 27, 28]. The intent of publishing this table is to provide PGAA and NAA practitioners with a reference consisting of Westcott g factors for a broad range of Maxwellian-spectrum average temperatures, obtained using the most up-to-date neutron-capture cross sections from ENDF/B-VIII.1. Table A1 includes several isotopes that display nearly- $1/v$ behavior, evident from $g_w \approx 1$ across the range of temperatures. Because these isotopes appear in other references cited in this paper, they were included here for completeness. It is notable that for several isotopes, including ^{132}Ba , ^{138}Ce , ^{163}Dy , ^{175}Lu , ^{180}Ta , and ^{186}Ta , the Westcott g -factor values in Table A1 differ from the values in the IAEA Database [1] by greater than 1%.

It is worth noting that the Westcott g factors in Table A1 should be treated with caution, particularly for highly-irregular nuclei, for the reasons outlined in Sec. 3.3. If an experimental neutron-energy spectrum is available, it should be used with the WestcottFactors or DeCE tools described in this work instead of a Maxwellian-distribution approximation, to ensure the Westcott g factors are accurate for the particular application.

Table 5

Westcott g factors calculated for select non- $1/v$ nuclei using Maxwellian neutron velocity distributions with various average temperatures T , as well as the reactor spectra described in Sec. 2.3. Cross sections were taken from ENDF/B-VIII.1, in the GNDS format for use with the `WestcottFactors` tool described in the text, and in the ENDF-6 format for use with DeCE. Percentage differences between the g_w values obtained using the two methods are included to facilitate comparison.

| Isotope | T (K) or Spectrum | g_w (WestcottFactors) | g_w (DeCE) | % Difference |
|-------------------|---------------------|-------------------------|--------------|--------------|
| ^{83}Kr | 100 | 1.002 | 1.003 | -0.1 |
| | 200 | 0.998 | 0.999 | -0.1 |
| | 293 | 0.995 | 0.996 | -0.1 |
| | 400 | 0.992 | 0.993 | -0.1 |
| | 500 | 0.989 | 0.990 | -0.1 |
| | 600 | 0.985 | 0.986 | -0.1 |
| | BRR cold | 1.003 | 1.004 | -0.1 |
| | BRR thermal | 0.958 | 0.959 | -0.1 |
| | FRM II cold | 1.001 | 1.002 | -0.1 |
| ^{115}In | 100 | 0.989 | 0.990 | -0.1 |
| | 200 | 1.014 | 1.015 | -0.1 |
| | 293 | 1.038 | 1.039 | -0.1 |
| | 400 | 1.067 | 1.068 | -0.1 |
| | 500 | 1.097 | 1.098 | -0.1 |
| | 600 | 1.128 | 1.129 | -0.1 |
| | BRR cold | 0.982 | 0.983 | -0.1 |
| | BRR thermal | 2.046 | 2.049 | -0.1 |
| | FRM II cold | 0.993 | 0.995 | -0.1 |
| ^{149}Sm | 100 | 0.893 | 0.895 | -0.3 |
| | 200 | 1.539 | 1.543 | -0.3 |
| | 293 | 2.134 | 2.139 | -0.2 |
| | 400 | 2.503 | 2.508 | -0.2 |
| | 500 | 2.593 | 2.598 | -0.2 |
| | 600 | 2.541 | 2.546 | -0.2 |
| | BRR cold | 0.799 | 0.801 | -0.3 |
| | BRR thermal | 0.776 | 0.778 | -0.3 |
| | FRM II cold | 1.082 | 1.085 | -0.2 |
| ^{151}Eu | 100 | 1.146 | 1.147 | -0.1 |
| | 200 | 0.954 | 0.956 | -0.2 |
| | 293 | 0.841 | 0.843 | -0.2 |
| | 400 | 0.765 | 0.766 | -0.2 |
| | 500 | 0.741 | 0.743 | -0.2 |
| | 600 | 0.763 | 0.764 | -0.2 |
| | BRR cold | 1.237 | 1.238 | -0.1 |
| | BRR thermal | 1.150 | 1.151 | -0.1 |
| | FRM II cold | 1.135 | 1.136 | -0.1 |
| ^{157}Gd | 100 | 0.912 | 0.913 | -0.2 |
| | 200 | 0.890 | 0.891 | -0.1 |
| | 293 | 0.802 | 0.804 | -0.1 |
| | 400 | 0.693 | 0.694 | -0.1 |
| | 500 | 0.603 | 0.603 | -0.1 |
| | 600 | 0.526 | 0.527 | -0.2 |
| | BRR cold | 0.869 | 0.871 | -0.2 |
| | BRR thermal | 0.833 | 0.835 | -0.2 |
| | FRM II cold | 0.872 | 0.873 | -0.1 |
| ^{176}Lu | 100 | 0.911 | 0.913 | -0.2 |
| | 200 | 1.432 | 1.436 | -0.3 |
| | 293 | 2.302 | 2.307 | -0.2 |
| | 400 | 3.330 | 3.338 | -0.2 |
| | 500 | 4.025 | 4.034 | -0.2 |
| | 600 | 4.426 | 4.435 | -0.2 |
| | BRR cold | 0.848 | 0.849 | -0.2 |
| | BRR thermal | 0.917 | 0.919 | -0.2 |
| | FRM II cold | 1.013 | 1.016 | -0.3 |

4. Summary

Computational methods for evaluating Westcott g factors were developed into the open-source `WestcottFactors` [17, 18] software tool, which allows users to specify an arbitrary neutron spectrum and calculate values of g_w for use in NAA and PGAA experiments. For users familiar with using DeCE to interact with ENDF data, modifications to that code package [19, 34] provide the same functionality for performing these calculations as the `WestcottFactors` tool. Tests of the two tools demonstrate consistency in their results, so users can choose to use the tool that best suits their needs for calculating Westcott g factors.

The results of testing these codes on a select number of irregular non- $1/v$ nuclei show that the Westcott g factors are sensitive to the choice of neutron spectrum, and certain low-energy neutron-capture cross section resonances. In the case of highly-irregular nuclei with multiple resonances below 5 eV, employing irregularity functions to approximate the calculation of Westcott g factors may result in significant differences when compared to the more accurate method of integrating over the full neutron-capture cross sections.

Most importantly, this study showed that Westcott g factors calculated with Maxwellian neutron velocity distributions can result in errors when approximating the actual g_w values obtained by integrating over the measured neutron spectra; this was demonstrated using experimentally-measured spectra from guided thermal- and cold-neutron PGAA beamlines at BRR and FRM II. This comparison demonstrates the utility of the open-source `WestcottFactors` software package, and the modifications to the DeCE tool, that have been made available as part of this work.

Acknowledgments

This work was supported at the Lawrence Berkeley National Laboratory under Contract No. DE-AC02-05CH11231 and at the Los Alamos National Laboratory under Contract No. 89233218CNA000001 for the U.S. Nuclear Data Program. Work at the University of California, Berkeley, was supported by the U.S. Department of Energy National Nuclear Security Administration through the Nuclear Science and Security Consortium under Award Number DE-NA0003996. The authors would like to express their gratitude to Laszlo Szentmiklósi, Tamas Belgya, and Zsolt Révay for providing neutron flux data from the Budapest Research Reactor and FRM II.

References

- [1] H. D. Choi, et al. (Eds.), Database of Prompt Gamma Rays from Slow Neutron Capture for Elemental Analysis, International Atomic Energy Agency, Vienna, Austria, 2007.
- [2] S. F. Mughabghab, Resonance Properties and Thermal Cross Sections $Z=1-102$, 6th Edition, Elsevier Science, 2018.
- [3] G. L. Molnár (Ed.), Handbook of Prompt Gamma Activation Analysis, Kluwer Academic, Dordrecht, the Netherlands, 2004.
- [4] R. B. Firestone, Renormalization of pile oscillator thermal neutron capture cross section data, Tech. Rep. INDC(USA)-109, International Atomic Energy Agency, Vienna, Austria (October 2021).
- [5] A. Trkov, et al., IRDFF-II: A new neutron metrology library, Nuclear Data Sheets 163 (2020) 1–108.
- [6] R. B. Firestone, Database of prompt gamma rays from slow neutron capture for elemental analysis, (International Atomic Energy Agency, Vienna, 2006).
URL <https://www-nds.iaea.org/pgaa/egaf.html>
- [7] A. M. Hurst, R. B. Firestone, E. V. Chmianski, pyEGAF: An open-source Python library for the evaluated gamma-ray activation file, Nuclear Instruments and Methods in Physics Research A 1067 (2023) 168715.
- [8] A. M. Hurst, pyEGAF (PyPI package).
URL <https://pypi.org/project/pyEGAF/>
- [9] C. H. Westcott, The specification of neutron flux and nuclear cross-sections in reactor calculations, Journal of Nuclear Energy 2 (1955) 59 – 76.
- [10] C. H. Westcott, Effective cross section values for well-moderated thermal reactor spectra, Tech. Rep. CRRP-960, Atomic Energy of Canada Limited, Chalk River, Ontario (1960).
- [11] D. A. Brown, et al., ENDF/B-VIII.0: The 8th major release of the nuclear reaction data library with CIELO-project cross sections, new standards and thermal scattering data, Nuclear Data Sheets 148 (2018) 1–142.
- [12] J. Byrne (Ed.), Neutrons, Nuclei, and Matter, Institute of Physics Publishing, Bristol and Philadelphia, 1994.
- [13] G. Nobre, D. Brown, R. Arcilla, R. Coles, B. Shu, Progress towards the ENDF/B-VIII.1 release, European Physics Journal Web of Conferences 294 (2024) 04004.
- [14] T. Kawano, DeCE: the ENDF-6 data interface and nuclear data evaluation assist code, Journal of Nuclear Science and Technology 56 (11) (2019) 1029 – 1035.
- [15] T. Kawano, DeCE (GitHub repository).
URL <https://github.com/toshihikokawano/DeCE>

- [16] D. Brown, B. Beck, C. Mattoon, T. Bailey, I. Thompson, J. L. Conlin, W. Haeck, M. White, M. Paris, M. Fleming, et al., Specifications for the Generalised Nuclear Database Structure (GNDS)-version 1.9, Tech. Rep. Technical Report NEA-7519, Organisation for Economic Cooperation and Development (2020).
- [17] D. A. Matters, A. M. Hurst, Westcott factors (GitHub repository).
URL <https://github.com/DMatters/WestcottFactors>
- [18] D. A. Matters, A. M. Hurst, WestcottFactors (PyPI package).
URL <https://pypi.org/project/westcott/>
- [19] T. Kawano, DeCE develop branch (GitHub repository).
URL <https://github.com/toshihikokawano/DeCE/tree/develop>
- [20] D. A. Brown, et al., ENDF-6 formats manual, Tech. Rep. BNL-224854-2023-INR, Cross Sections Evaluations Working Group (September 2023).
- [21] W. McKinney, Data structures for statistical computing in Python, in: S. van der Walt, J. Millman (Eds.), Proceedings of the 9th Python in Science Conference, 2010, pp. 56 – 61.
- [22] C. Mattoon, B. Beck, G. Godfree, Managing and processing nuclear data libraries with FUDGE, EPJ Web of Conferences 284 (2023) 14010.
- [23] C. Mattoon, For updating data and generating evaluations (FUDGE): LLNL code for managing nuclear data (GitHub repository).
URL <https://github.com/LLNL/fudge>
- [24] P. Virtanen, SciPy 1.0 Contributors, SciPy 1.0: Fundamental Algorithms for Scientific Computing in Python, *Nature Methods* 17 (2020) 261–272.
- [25] A. L. Nichols, D. L. Aldama, M. Verpelli, Database extensions, August 2008, in: Handbook of Nuclear Data for Safeguards, no. INDC(NDS)-0534, IAEA, Vienna, Austria, 2008.
- [26] R. van Sluijs, A. Stopic, R. Jacimovic, Evaluation of Westcott $g(t_n)$ -factors used in k_0 -NAA for "non-1/v" (n, γ) reactions, *Journal of Radioanalytical and Nuclear Chemistry* 306 (2015) 579–587.
- [27] N. E. Holden, Temperature dependence of the Westcott *g*-factor for neutron reactions in activation analysis (IUPAC technical report), *Pure and Applied Chemistry* 71 (12) (1999) 2309–2315.
- [28] B. Pritychenko, Tables of neutron thermal cross sections, Westcott factors, resonance integrals, Maxwellian averaged cross sections, astrophysical reaction rates, and *r*-process abundances calculated from the ENDF/B-VIII.1, JEFF-3.3, JENDL-5.0, BROND-3.1, and CENDL-3.2 evaluated data libraries, *Atomic Data and Nuclear Data Tables* 163 (2025) 101708.
- [29] M. Chand, S. Bagchi, B. H. Khan, Determination of Westcott *g*-factors for the assay of non-1/v nuclides using k_0 -NAA, *Applied Radiation and Isotopes* 217 (2025) 111666.
- [30] T. Belgya, Prompt gamma activation analysis at the Budapest Research Reactor, *Physics Procedia* 31 (2012) 99–109.
- [31] T. Belgya, Z. Kis, L. Szentmiklósi, Neutron flux characterization of the cold beam PGAA-NIPS facility at the Budapest research reactor, *Nuclear Data Sheets* 119 (2014) 419–421.
- [32] Z. Révay, T. Belgya, Z. Kasztovszky, J. L. Weil, G. L. Molnár, Cold neutron PGAA facility at Budapest, *Nuclear Instruments and Methods in Physics Research B* 213 (2004) 385–388.
- [33] P. Kudejova, G. Meierhofer, K. Zeitelhack, J. Jolie, R. Schulze, A. Türler, T. Materna, The new PGAA and PGAI facility at the research reactor FRM II in Garching near Munich, *Journal of Radioanalytical and Nuclear Chemistry* 278 (3) (2008) 691–695.
- [34] D. Matters, T. Kawano, Fork to DeCE develop branch (GitHub repository).
URL https://github.com/DMatters/DeCE_g-Factor/tree/develop
- [35] C. L. Dunford, Organisation for Economic Co-Operation and Development, Nuclear Energy Agency - OECD/NEA, Inter: ENDF/B thermal cross-sections, resonance integrals, *g*-factors calculation.
URL <https://inis.iaea.org/records/fqpqg-d3r21>
- [36] C. L. Dunford, Evaluated nuclear data file, ENDF/B-VI, in: S. M. Qaim (Ed.), *Nuclear Data for Science and Technology*, Springer Berlin Heidelberg, Berlin, Heidelberg, 1992, pp. 788–792.

Appendix: Maxwellian-spectrum Westcott g Factors for Irregular Nuclei

Table A1

Maxwellian-distribution Westcott g factors at various temperatures T for non- $1/v$ nuclei listed in References [1, 3, 26, 27, 28], calculated using the cross-section integration method in the `WestcottFactors` toolkit [17, 18], with cross sections taken from ENDF/B-VIII.1 [11, 13].

| T (K) | ^{30}Si | ^{36}S | ^{36}Ar | ^{38}Ar | ^{83}Kr | ^{87}Sr | ^{93}Nb | ^{103}Rh | ^{105}Pd | ^{107}Ag | ^{109}Ag | ^{111}Cd | ^{113}Cd |
|---------|------------------|-----------------|------------------|------------------|------------------|------------------|------------------|-------------------|-------------------|-------------------|-------------------|-------------------|-------------------|
| 20 | 1.000 | 0.804 | 1.159 | 1.304 | 1.004 | 0.990 | 1.000 | 0.966 | 1.002 | 1.003 | 0.992 | 1.001 | 0.789 |
| 40 | 1.000 | 0.860 | 1.101 | 1.257 | 1.004 | 0.992 | 1.000 | 0.971 | 1.002 | 1.002 | 0.994 | 1.001 | 0.819 |
| 60 | 1.000 | 0.895 | 1.064 | 1.182 | 1.003 | 0.993 | 1.000 | 0.976 | 1.001 | 1.002 | 0.995 | 1.001 | 0.852 |
| 80 | 1.000 | 0.921 | 1.044 | 1.132 | 1.002 | 0.995 | 1.000 | 0.982 | 1.001 | 1.002 | 0.996 | 1.001 | 0.888 |
| 100 | 1.000 | 0.942 | 1.032 | 1.099 | 1.002 | 0.996 | 1.000 | 0.987 | 1.001 | 1.001 | 0.997 | 1.000 | 0.927 |
| 120 | 1.000 | 0.960 | 1.025 | 1.077 | 1.001 | 0.998 | 1.000 | 0.993 | 1.001 | 1.001 | 0.999 | 1.000 | 0.971 |
| 140 | 1.000 | 0.975 | 1.020 | 1.062 | 1.000 | 0.999 | 1.000 | 0.998 | 1.000 | 1.000 | 1.000 | 1.000 | 1.021 |
| 160 | 1.000 | 0.988 | 1.017 | 1.052 | 1.000 | 1.001 | 1.000 | 1.004 | 1.000 | 1.000 | 1.001 | 1.000 | 1.076 |
| 180 | 1.000 | 1.001 | 1.015 | 1.044 | 0.999 | 1.002 | 1.000 | 1.010 | 1.000 | 0.999 | 1.002 | 1.000 | 1.139 |
| 200 | 1.000 | 1.012 | 1.013 | 1.038 | 0.998 | 1.004 | 1.000 | 1.016 | 1.000 | 0.999 | 1.004 | 0.999 | 1.209 |
| 220 | 1.000 | 1.022 | 1.012 | 1.033 | 0.998 | 1.006 | 1.000 | 1.022 | 0.999 | 0.998 | 1.005 | 0.999 | 1.286 |
| 240 | 1.000 | 1.032 | 1.011 | 1.029 | 0.997 | 1.007 | 0.999 | 1.028 | 0.999 | 0.998 | 1.006 | 0.999 | 1.371 |
| 260 | 1.000 | 1.041 | 1.011 | 1.026 | 0.996 | 1.009 | 0.999 | 1.034 | 0.999 | 0.997 | 1.007 | 0.999 | 1.463 |
| 280 | 1.000 | 1.049 | 1.010 | 1.024 | 0.996 | 1.010 | 0.999 | 1.040 | 0.999 | 0.997 | 1.009 | 0.999 | 1.560 |
| 293 | 1.000 | 1.054 | 1.010 | 1.023 | 0.995 | 1.011 | 0.999 | 1.044 | 0.998 | 0.996 | 1.010 | 0.999 | 1.626 |
| 300 | 1.000 | 1.057 | 1.010 | 1.022 | 0.995 | 1.012 | 0.999 | 1.046 | 0.998 | 0.996 | 1.010 | 0.998 | 1.662 |
| 320 | 1.000 | 1.064 | 1.009 | 1.020 | 0.994 | 1.014 | 0.999 | 1.052 | 0.998 | 0.996 | 1.011 | 0.998 | 1.767 |
| 340 | 1.000 | 1.071 | 1.009 | 1.019 | 0.994 | 1.015 | 0.999 | 1.059 | 0.998 | 0.995 | 1.013 | 0.998 | 1.875 |
| 360 | 1.000 | 1.078 | 1.009 | 1.018 | 0.993 | 1.017 | 0.999 | 1.065 | 0.998 | 0.995 | 1.014 | 0.998 | 1.982 |
| 380 | 1.000 | 1.084 | 1.008 | 1.017 | 0.993 | 1.018 | 0.999 | 1.072 | 0.997 | 0.994 | 1.015 | 0.998 | 2.090 |
| 400 | 1.000 | 1.090 | 1.008 | 1.016 | 0.992 | 1.020 | 0.999 | 1.079 | 0.997 | 0.994 | 1.017 | 0.998 | 2.196 |
| 420 | 1.000 | 1.096 | 1.008 | 1.015 | 0.991 | 1.022 | 0.999 | 1.086 | 0.997 | 0.993 | 1.018 | 0.997 | 2.299 |
| 440 | 1.000 | 1.102 | 1.008 | 1.014 | 0.991 | 1.023 | 0.999 | 1.093 | 0.997 | 0.993 | 1.019 | 0.997 | 2.400 |
| 460 | 1.000 | 1.107 | 1.008 | 1.014 | 0.990 | 1.025 | 0.999 | 1.100 | 0.996 | 0.992 | 1.020 | 0.997 | 2.496 |
| 480 | 1.000 | 1.112 | 1.008 | 1.013 | 0.989 | 1.027 | 0.999 | 1.107 | 0.996 | 0.992 | 1.022 | 0.997 | 2.589 |
| 500 | 1.000 | 1.117 | 1.008 | 1.013 | 0.989 | 1.028 | 0.999 | 1.114 | 0.996 | 0.991 | 1.023 | 0.997 | 2.676 |
| 520 | 1.000 | 1.122 | 1.008 | 1.012 | 0.988 | 1.030 | 0.999 | 1.122 | 0.996 | 0.991 | 1.024 | 0.996 | 2.759 |
| 540 | 1.000 | 1.127 | 1.008 | 1.012 | 0.987 | 1.032 | 0.999 | 1.129 | 0.995 | 0.990 | 1.026 | 0.996 | 2.837 |
| 560 | 1.000 | 1.131 | 1.007 | 1.011 | 0.987 | 1.033 | 0.999 | 1.137 | 0.995 | 0.990 | 1.027 | 0.996 | 2.909 |
| 580 | 1.000 | 1.136 | 1.007 | 1.011 | 0.986 | 1.035 | 0.999 | 1.145 | 0.995 | 0.989 | 1.028 | 0.996 | 2.977 |
| 600 | 1.000 | 1.140 | 1.007 | 1.011 | 0.985 | 1.037 | 0.998 | 1.153 | 0.995 | 0.989 | 1.030 | 0.996 | 3.039 |

| <i>T</i> (K) | ^{113}In | ^{115}In | ^{121}Sb | ^{123}Te | ^{124}Xe | ^{135}Xe | ^{132}Ba | ^{133}Cs | ^{138}Ce | ^{143}Nd | ^{148}Pm | ^{149}Sm | ^{151}Sm |
|--------------|-------------------|-------------------|-------------------|-------------------|-------------------|-------------------|-------------------|-------------------|-------------------|-------------------|-------------------|-------------------|-------------------|
| 20 | 0.981 | 0.971 | 0.994 | 0.982 | 0.994 | 0.699 | 1.000 | 0.996 | 1.003 | 1.007 | 1.000 | 0.639 | 1.332 |
| 40 | 0.984 | 0.975 | 0.995 | 0.985 | 0.995 | 0.740 | 1.000 | 0.997 | 1.002 | 1.006 | 1.000 | 0.685 | 1.273 |
| 60 | 0.987 | 0.980 | 0.996 | 0.988 | 0.996 | 0.786 | 1.000 | 0.998 | 1.002 | 1.005 | 1.000 | 0.741 | 1.219 |
| 80 | 0.990 | 0.985 | 0.997 | 0.990 | 0.997 | 0.837 | 1.000 | 0.998 | 1.002 | 1.004 | 1.000 | 0.809 | 1.170 |
| 100 | 0.993 | 0.989 | 0.998 | 0.993 | 0.998 | 0.892 | 1.000 | 0.999 | 1.001 | 1.003 | 1.000 | 0.893 | 1.124 |
| 120 | 0.996 | 0.994 | 0.999 | 0.996 | 0.999 | 0.948 | 1.000 | 0.999 | 1.001 | 1.002 | 1.000 | 0.995 | 1.082 |
| 140 | 0.999 | 0.999 | 1.000 | 0.999 | 1.000 | 1.004 | 1.000 | 1.000 | 1.000 | 1.001 | 1.000 | 1.115 | 1.043 |
| 160 | 1.003 | 1.004 | 1.001 | 1.002 | 1.001 | 1.058 | 1.000 | 1.000 | 1.000 | 1.000 | 1.000 | 1.250 | 1.007 |
| 180 | 1.006 | 1.009 | 1.002 | 1.005 | 1.002 | 1.109 | 1.000 | 1.001 | 1.000 | 0.999 | 1.000 | 1.393 | 0.974 |
| 200 | 1.009 | 1.014 | 1.002 | 1.008 | 1.003 | 1.154 | 1.000 | 1.001 | 0.999 | 0.997 | 1.000 | 1.539 | 0.942 |
| 220 | 1.012 | 1.019 | 1.003 | 1.012 | 1.004 | 1.194 | 1.000 | 1.002 | 0.999 | 0.996 | 1.000 | 1.683 | 0.913 |
| 240 | 1.016 | 1.024 | 1.004 | 1.015 | 1.005 | 1.228 | 1.000 | 1.003 | 0.998 | 0.995 | 1.000 | 1.820 | 0.885 |
| 260 | 1.019 | 1.029 | 1.005 | 1.018 | 1.006 | 1.257 | 1.000 | 1.003 | 0.998 | 0.994 | 1.000 | 1.948 | 0.859 |
| 280 | 1.023 | 1.034 | 1.006 | 1.021 | 1.007 | 1.280 | 1.000 | 1.004 | 0.998 | 0.993 | 1.000 | 2.065 | 0.834 |
| 293 | 1.025 | 1.038 | 1.007 | 1.023 | 1.008 | 1.292 | 1.000 | 1.004 | 0.997 | 0.993 | 1.000 | 2.134 | 0.819 |
| 300 | 1.026 | 1.040 | 1.007 | 1.024 | 1.008 | 1.298 | 1.000 | 1.004 | 0.997 | 0.992 | 1.000 | 2.169 | 0.811 |
| 320 | 1.029 | 1.045 | 1.008 | 1.027 | 1.009 | 1.311 | 1.000 | 1.005 | 0.997 | 0.991 | 1.000 | 2.260 | 0.789 |
| 340 | 1.033 | 1.051 | 1.009 | 1.030 | 1.011 | 1.319 | 1.000 | 1.006 | 0.996 | 0.990 | 1.000 | 2.338 | 0.768 |
| 360 | 1.036 | 1.056 | 1.010 | 1.034 | 1.012 | 1.324 | 1.000 | 1.006 | 0.996 | 0.989 | 1.000 | 2.404 | 0.748 |
| 380 | 1.040 | 1.062 | 1.011 | 1.037 | 1.013 | 1.325 | 1.000 | 1.007 | 0.996 | 0.988 | 1.000 | 2.459 | 0.730 |
| 400 | 1.044 | 1.067 | 1.011 | 1.040 | 1.014 | 1.323 | 1.000 | 1.007 | 0.995 | 0.987 | 1.000 | 2.503 | 0.712 |
| 420 | 1.047 | 1.073 | 1.012 | 1.044 | 1.015 | 1.319 | 1.000 | 1.008 | 0.995 | 0.986 | 1.000 | 2.537 | 0.695 |
| 440 | 1.051 | 1.079 | 1.013 | 1.047 | 1.016 | 1.312 | 1.000 | 1.009 | 0.995 | 0.985 | 1.000 | 2.562 | 0.679 |
| 460 | 1.055 | 1.085 | 1.014 | 1.050 | 1.017 | 1.304 | 0.999 | 1.009 | 0.994 | 0.984 | 1.000 | 2.579 | 0.663 |
| 480 | 1.058 | 1.091 | 1.015 | 1.054 | 1.018 | 1.293 | 0.999 | 1.010 | 0.994 | 0.983 | 1.000 | 2.589 | 0.648 |
| 500 | 1.062 | 1.097 | 1.016 | 1.057 | 1.019 | 1.281 | 0.999 | 1.010 | 0.993 | 0.982 | 1.000 | 2.593 | 0.634 |
| 520 | 1.066 | 1.103 | 1.017 | 1.061 | 1.020 | 1.268 | 0.999 | 1.011 | 0.993 | 0.981 | 1.000 | 2.591 | 0.621 |
| 540 | 1.070 | 1.109 | 1.018 | 1.064 | 1.022 | 1.254 | 0.999 | 1.012 | 0.993 | 0.980 | 1.000 | 2.584 | 0.608 |
| 560 | 1.074 | 1.115 | 1.019 | 1.067 | 1.023 | 1.239 | 0.999 | 1.012 | 0.992 | 0.979 | 1.000 | 2.573 | 0.595 |
| 580 | 1.078 | 1.122 | 1.020 | 1.071 | 1.024 | 1.224 | 0.999 | 1.013 | 0.992 | 0.978 | 1.000 | 2.558 | 0.583 |
| 600 | 1.082 | 1.128 | 1.021 | 1.075 | 1.025 | 1.208 | 0.999 | 1.013 | 0.991 | 0.977 | 1.000 | 2.541 | 0.572 |

| <i>T</i> (K) | ^{152}Sm | ^{151}Eu | ^{152}Eu | ^{153}Eu | ^{154}Eu | ^{155}Eu | ^{152}Gd | ^{155}Gd | ^{157}Gd | ^{159}Tb | ^{156}Dy | ^{158}Dy | ^{160}Dy |
|--------------|-------------------|-------------------|-------------------|-------------------|-------------------|-------------------|-------------------|-------------------|-------------------|-------------------|-------------------|-------------------|-------------------|
| 20 | 0.995 | 1.388 | 1.287 | 1.029 | 0.819 | 0.988 | 1.007 | 0.844 | 0.801 | 0.998 | 0.987 | 1.020 | 0.991 |
| 40 | 0.995 | 1.317 | 1.237 | 1.025 | 0.845 | 0.989 | 1.006 | 0.878 | 0.839 | 0.999 | 0.989 | 1.017 | 0.992 |
| 60 | 0.996 | 1.254 | 1.191 | 1.020 | 0.873 | 0.991 | 1.005 | 0.905 | 0.872 | 0.999 | 0.991 | 1.014 | 0.993 |
| 80 | 0.997 | 1.197 | 1.148 | 1.016 | 0.904 | 0.993 | 1.004 | 0.922 | 0.896 | 0.999 | 0.993 | 1.011 | 0.995 |
| 100 | 0.998 | 1.146 | 1.108 | 1.011 | 0.937 | 0.996 | 1.003 | 0.930 | 0.912 | 1.000 | 0.995 | 1.007 | 0.996 |
| 120 | 0.999 | 1.100 | 1.070 | 1.007 | 0.973 | 0.999 | 1.002 | 0.930 | 0.919 | 1.000 | 0.997 | 1.004 | 0.998 |
| 140 | 1.000 | 1.058 | 1.035 | 1.002 | 1.012 | 1.002 | 1.000 | 0.924 | 0.919 | 1.000 | 0.999 | 1.001 | 0.999 |
| 160 | 1.001 | 1.020 | 1.002 | 0.998 | 1.055 | 1.006 | 0.999 | 0.913 | 0.914 | 1.000 | 1.001 | 0.998 | 1.001 |
| 180 | 1.001 | 0.985 | 0.970 | 0.994 | 1.102 | 1.010 | 0.998 | 0.897 | 0.904 | 1.001 | 1.004 | 0.995 | 1.003 |
| 200 | 1.002 | 0.954 | 0.941 | 0.990 | 1.153 | 1.014 | 0.997 | 0.880 | 0.890 | 1.001 | 1.006 | 0.992 | 1.004 |
| 220 | 1.003 | 0.925 | 0.913 | 0.985 | 1.209 | 1.019 | 0.996 | 0.860 | 0.874 | 1.001 | 1.008 | 0.989 | 1.006 |
| 240 | 1.004 | 0.899 | 0.887 | 0.981 | 1.268 | 1.024 | 0.995 | 0.839 | 0.855 | 1.002 | 1.010 | 0.986 | 1.007 |
| 260 | 1.005 | 0.875 | 0.862 | 0.977 | 1.331 | 1.030 | 0.994 | 0.817 | 0.836 | 1.002 | 1.012 | 0.983 | 1.009 |
| 280 | 1.006 | 0.854 | 0.839 | 0.973 | 1.397 | 1.036 | 0.993 | 0.795 | 0.816 | 1.002 | 1.015 | 0.980 | 1.010 |
| 293 | 1.006 | 0.841 | 0.824 | 0.971 | 1.441 | 1.040 | 0.992 | 0.780 | 0.802 | 1.003 | 1.016 | 0.978 | 1.011 |
| 300 | 1.007 | 0.834 | 0.817 | 0.969 | 1.465 | 1.042 | 0.992 | 0.772 | 0.795 | 1.003 | 1.017 | 0.977 | 1.012 |
| 320 | 1.007 | 0.816 | 0.795 | 0.966 | 1.535 | 1.049 | 0.991 | 0.750 | 0.774 | 1.003 | 1.019 | 0.974 | 1.014 |
| 340 | 1.008 | 0.801 | 0.775 | 0.962 | 1.606 | 1.057 | 0.990 | 0.729 | 0.754 | 1.003 | 1.021 | 0.971 | 1.015 |
| 360 | 1.009 | 0.787 | 0.756 | 0.958 | 1.678 | 1.065 | 0.989 | 0.708 | 0.733 | 1.004 | 1.024 | 0.968 | 1.017 |
| 380 | 1.010 | 0.775 | 0.738 | 0.954 | 1.749 | 1.074 | 0.988 | 0.687 | 0.713 | 1.004 | 1.026 | 0.965 | 1.019 |
| 400 | 1.011 | 0.765 | 0.720 | 0.951 | 1.819 | 1.083 | 0.986 | 0.667 | 0.693 | 1.005 | 1.028 | 0.962 | 1.020 |
| 420 | 1.012 | 0.756 | 0.704 | 0.947 | 1.888 | 1.093 | 0.985 | 0.647 | 0.674 | 1.005 | 1.031 | 0.959 | 1.022 |
| 440 | 1.013 | 0.750 | 0.688 | 0.943 | 1.955 | 1.105 | 0.984 | 0.629 | 0.655 | 1.005 | 1.033 | 0.956 | 1.024 |
| 460 | 1.013 | 0.745 | 0.672 | 0.940 | 2.019 | 1.117 | 0.983 | 0.610 | 0.637 | 1.006 | 1.035 | 0.953 | 1.026 |
| 480 | 1.014 | 0.742 | 0.658 | 0.936 | 2.081 | 1.130 | 0.982 | 0.593 | 0.620 | 1.006 | 1.038 | 0.951 | 1.027 |
| 500 | 1.015 | 0.741 | 0.643 | 0.933 | 2.141 | 1.145 | 0.981 | 0.576 | 0.603 | 1.006 | 1.040 | 0.948 | 1.029 |
| 520 | 1.016 | 0.742 | 0.630 | 0.929 | 2.197 | 1.162 | 0.980 | 0.560 | 0.586 | 1.007 | 1.042 | 0.945 | 1.031 |
| 540 | 1.017 | 0.744 | 0.617 | 0.926 | 2.250 | 1.180 | 0.979 | 0.544 | 0.570 | 1.007 | 1.045 | 0.942 | 1.033 |
| 560 | 1.018 | 0.749 | 0.604 | 0.923 | 2.300 | 1.200 | 0.978 | 0.529 | 0.555 | 1.007 | 1.047 | 0.940 | 1.034 |
| 580 | 1.019 | 0.755 | 0.592 | 0.919 | 2.347 | 1.223 | 0.977 | 0.515 | 0.540 | 1.008 | 1.050 | 0.937 | 1.036 |
| 600 | 1.020 | 0.763 | 0.581 | 0.916 | 2.391 | 1.248 | 0.976 | 0.501 | 0.526 | 1.008 | 1.052 | 0.934 | 1.038 |

| <i>T</i> (K) | ^{161}Dy | ^{162}Dy | ^{163}Dy | ^{164}Dy | ^{167}Er | ^{169}Tm | ^{168}Yb | ^{175}Lu | ^{176}Lu | ^{174}Hf | ^{176}Hf | ^{177}Hf | ^{178}Hf |
|--------------|-------------------|-------------------|-------------------|-------------------|-------------------|-------------------|-------------------|-------------------|-------------------|-------------------|-------------------|-------------------|-------------------|
| 20 | 1.015 | 0.992 | 0.982 | 1.023 | 0.921 | 0.992 | 0.928 | 0.996 | 0.726 | 1.044 | 0.997 | 0.970 | 0.995 |
| 40 | 1.013 | 0.993 | 0.985 | 1.020 | 0.933 | 0.993 | 0.939 | 0.997 | 0.764 | 1.037 | 0.997 | 0.975 | 0.996 |
| 60 | 1.011 | 0.995 | 0.988 | 1.016 | 0.945 | 0.995 | 0.950 | 0.998 | 0.806 | 1.030 | 0.998 | 0.980 | 0.997 |
| 80 | 1.008 | 0.996 | 0.991 | 1.012 | 0.958 | 0.996 | 0.962 | 0.998 | 0.854 | 1.023 | 0.998 | 0.984 | 0.997 |
| 100 | 1.006 | 0.997 | 0.993 | 1.009 | 0.971 | 0.997 | 0.974 | 0.999 | 0.911 | 1.017 | 0.999 | 0.989 | 0.998 |
| 120 | 1.004 | 0.998 | 0.996 | 1.005 | 0.985 | 0.999 | 0.986 | 0.999 | 0.980 | 1.010 | 0.999 | 0.994 | 0.999 |
| 140 | 1.001 | 1.000 | 0.999 | 1.001 | 0.999 | 1.000 | 0.999 | 1.000 | 1.063 | 1.003 | 1.000 | 0.999 | 1.000 |
| 160 | 0.999 | 1.001 | 1.003 | 0.998 | 1.014 | 1.001 | 1.012 | 1.001 | 1.165 | 0.997 | 1.000 | 1.004 | 1.000 |
| 180 | 0.997 | 1.002 | 1.006 | 0.994 | 1.030 | 1.002 | 1.025 | 1.001 | 1.288 | 0.990 | 1.001 | 1.009 | 1.001 |
| 200 | 0.994 | 1.003 | 1.009 | 0.991 | 1.046 | 1.004 | 1.039 | 1.002 | 1.432 | 0.984 | 1.001 | 1.014 | 1.002 |
| 220 | 0.992 | 1.005 | 1.012 | 0.987 | 1.063 | 1.005 | 1.054 | 1.003 | 1.596 | 0.978 | 1.002 | 1.020 | 1.003 |
| 240 | 0.990 | 1.006 | 1.015 | 0.984 | 1.080 | 1.006 | 1.068 | 1.003 | 1.776 | 0.972 | 1.002 | 1.025 | 1.003 |
| 260 | 0.988 | 1.007 | 1.018 | 0.981 | 1.099 | 1.008 | 1.084 | 1.004 | 1.969 | 0.966 | 1.003 | 1.030 | 1.004 |
| 280 | 0.985 | 1.008 | 1.022 | 0.977 | 1.118 | 1.009 | 1.100 | 1.004 | 2.169 | 0.960 | 1.004 | 1.036 | 1.005 |
| 293 | 0.984 | 1.009 | 1.024 | 0.975 | 1.131 | 1.010 | 1.111 | 1.005 | 2.302 | 0.956 | 1.004 | 1.039 | 1.005 |
| 300 | 0.983 | 1.010 | 1.025 | 0.974 | 1.139 | 1.010 | 1.116 | 1.005 | 2.373 | 0.954 | 1.004 | 1.041 | 1.005 |
| 320 | 0.981 | 1.011 | 1.028 | 0.970 | 1.161 | 1.012 | 1.134 | 1.006 | 2.577 | 0.948 | 1.005 | 1.047 | 1.006 |
| 340 | 0.979 | 1.012 | 1.032 | 0.967 | 1.184 | 1.013 | 1.152 | 1.006 | 2.777 | 0.942 | 1.005 | 1.052 | 1.007 |
| 360 | 0.977 | 1.014 | 1.035 | 0.964 | 1.210 | 1.014 | 1.171 | 1.007 | 2.971 | 0.937 | 1.006 | 1.058 | 1.008 |
| 380 | 0.975 | 1.015 | 1.038 | 0.961 | 1.237 | 1.016 | 1.190 | 1.008 | 3.156 | 0.931 | 1.006 | 1.064 | 1.008 |
| 400 | 0.972 | 1.016 | 1.042 | 0.957 | 1.267 | 1.017 | 1.211 | 1.008 | 3.330 | 0.926 | 1.007 | 1.070 | 1.009 |
| 420 | 0.970 | 1.017 | 1.045 | 0.954 | 1.300 | 1.019 | 1.234 | 1.009 | 3.494 | 0.920 | 1.007 | 1.076 | 1.010 |
| 440 | 0.968 | 1.019 | 1.049 | 0.951 | 1.337 | 1.020 | 1.258 | 1.009 | 3.645 | 0.915 | 1.008 | 1.082 | 1.011 |
| 460 | 0.966 | 1.020 | 1.053 | 0.948 | 1.377 | 1.021 | 1.283 | 1.010 | 3.784 | 0.910 | 1.009 | 1.089 | 1.011 |
| 480 | 0.964 | 1.021 | 1.056 | 0.945 | 1.422 | 1.023 | 1.311 | 1.011 | 3.911 | 0.904 | 1.009 | 1.095 | 1.012 |
| 500 | 0.962 | 1.023 | 1.060 | 0.942 | 1.472 | 1.024 | 1.342 | 1.011 | 4.025 | 0.899 | 1.010 | 1.101 | 1.013 |
| 520 | 0.960 | 1.024 | 1.064 | 0.938 | 1.528 | 1.026 | 1.376 | 1.012 | 4.127 | 0.894 | 1.010 | 1.108 | 1.014 |
| 540 | 0.958 | 1.025 | 1.067 | 0.935 | 1.589 | 1.027 | 1.413 | 1.013 | 4.218 | 0.889 | 1.011 | 1.115 | 1.014 |
| 560 | 0.956 | 1.027 | 1.071 | 0.932 | 1.656 | 1.028 | 1.455 | 1.013 | 4.298 | 0.884 | 1.011 | 1.122 | 1.015 |
| 580 | 0.954 | 1.028 | 1.075 | 0.929 | 1.731 | 1.030 | 1.501 | 1.014 | 4.367 | 0.879 | 1.012 | 1.129 | 1.016 |
| 600 | 0.952 | 1.029 | 1.079 | 0.926 | 1.812 | 1.031 | 1.553 | 1.015 | 4.426 | 0.874 | 1.012 | 1.136 | 1.017 |

Westcott *g* Factors Extended to Arbitrary Neutron Energy Spectra

| <i>T</i> (K) | ^{179}Hf | ^{180}Hf | ^{180}Ta | ^{181}Ta | ^{182}Ta | ^{180}W | ^{182}W | ^{185}Re | ^{187}Re | ^{186}Os | ^{187}Os | ^{191}Ir |
|--------------|-------------------|-------------------|-------------------|-------------------|-------------------|------------------|------------------|-------------------|-------------------|-------------------|-------------------|-------------------|
| 20 | 1.005 | 1.001 | 0.975 | 0.995 | 0.736 | 1.005 | 0.995 | 0.993 | 1.010 | 1.039 | 1.031 | 1.018 |
| 40 | 1.004 | 1.001 | 0.953 | 0.996 | 0.772 | 1.004 | 0.996 | 0.994 | 1.009 | 1.032 | 1.026 | 1.015 |
| 60 | 1.003 | 1.001 | 0.937 | 0.996 | 0.813 | 1.004 | 0.997 | 0.995 | 1.007 | 1.026 | 1.021 | 1.012 |
| 80 | 1.003 | 1.000 | 0.938 | 0.997 | 0.859 | 1.003 | 0.997 | 0.996 | 1.006 | 1.020 | 1.016 | 1.010 |
| 100 | 1.002 | 1.000 | 0.946 | 0.998 | 0.913 | 1.002 | 0.998 | 0.997 | 1.004 | 1.014 | 1.012 | 1.007 |
| 120 | 1.001 | 1.000 | 0.955 | 0.999 | 0.977 | 1.001 | 0.999 | 0.998 | 1.002 | 1.009 | 1.007 | 1.005 |
| 140 | 1.001 | 1.000 | 0.963 | 1.000 | 1.053 | 1.000 | 0.999 | 1.000 | 1.001 | 1.003 | 1.002 | 1.002 |
| 160 | 1.000 | 1.000 | 0.969 | 1.001 | 1.146 | 0.999 | 1.000 | 1.001 | 0.999 | 0.997 | 0.998 | 1.000 |
| 180 | 0.999 | 1.000 | 0.973 | 1.002 | 1.257 | 0.998 | 1.001 | 1.002 | 0.998 | 0.992 | 0.993 | 0.998 |
| 200 | 0.998 | 1.000 | 0.974 | 1.003 | 1.387 | 0.998 | 1.002 | 1.003 | 0.996 | 0.986 | 0.989 | 0.997 |
| 220 | 0.998 | 1.000 | 0.974 | 1.004 | 1.534 | 0.997 | 1.002 | 1.004 | 0.995 | 0.981 | 0.984 | 0.995 |
| 240 | 0.997 | 0.999 | 0.973 | 1.004 | 1.698 | 0.996 | 1.003 | 1.006 | 0.993 | 0.975 | 0.980 | 0.994 |
| 260 | 0.996 | 0.999 | 0.971 | 1.005 | 1.874 | 0.995 | 1.004 | 1.007 | 0.992 | 0.970 | 0.975 | 0.993 |
| 280 | 0.996 | 0.999 | 0.967 | 1.006 | 2.058 | 0.994 | 1.005 | 1.008 | 0.990 | 0.965 | 0.971 | 0.992 |
| 293 | 0.995 | 0.999 | 0.965 | 1.007 | 2.181 | 0.994 | 1.005 | 1.009 | 0.989 | 0.961 | 0.968 | 0.991 |
| 300 | 0.995 | 0.999 | 0.964 | 1.007 | 2.248 | 0.993 | 1.006 | 1.010 | 0.988 | 0.960 | 0.967 | 0.991 |
| 320 | 0.994 | 0.999 | 0.959 | 1.008 | 2.439 | 0.993 | 1.006 | 1.011 | 0.987 | 0.954 | 0.963 | 0.990 |
| 340 | 0.994 | 0.999 | 0.955 | 1.009 | 2.628 | 0.992 | 1.007 | 1.012 | 0.985 | 0.949 | 0.958 | 0.990 |
| 360 | 0.993 | 0.999 | 0.951 | 1.010 | 2.813 | 0.991 | 1.008 | 1.014 | 0.984 | 0.944 | 0.954 | 0.990 |
| 380 | 0.992 | 0.998 | 0.946 | 1.011 | 2.991 | 0.990 | 1.009 | 1.015 | 0.982 | 0.939 | 0.950 | 0.990 |
| 400 | 0.992 | 0.998 | 0.942 | 1.012 | 3.161 | 0.989 | 1.009 | 1.016 | 0.981 | 0.935 | 0.946 | 0.990 |
| 420 | 0.991 | 0.998 | 0.939 | 1.013 | 3.322 | 0.989 | 1.010 | 1.018 | 0.979 | 0.930 | 0.942 | 0.991 |
| 440 | 0.990 | 0.998 | 0.935 | 1.014 | 3.472 | 0.988 | 1.011 | 1.019 | 0.978 | 0.925 | 0.938 | 0.992 |
| 460 | 0.990 | 0.998 | 0.932 | 1.015 | 3.611 | 0.987 | 1.012 | 1.021 | 0.976 | 0.920 | 0.934 | 0.994 |
| 480 | 0.989 | 0.998 | 0.929 | 1.016 | 3.739 | 0.986 | 1.013 | 1.022 | 0.975 | 0.916 | 0.930 | 0.995 |
| 500 | 0.988 | 0.998 | 0.927 | 1.016 | 3.856 | 0.985 | 1.013 | 1.023 | 0.973 | 0.911 | 0.926 | 0.998 |
| 520 | 0.988 | 0.997 | 0.926 | 1.017 | 3.961 | 0.985 | 1.014 | 1.025 | 0.972 | 0.906 | 0.922 | 1.001 |
| 540 | 0.987 | 0.997 | 0.925 | 1.018 | 4.056 | 0.984 | 1.015 | 1.026 | 0.971 | 0.902 | 0.919 | 1.004 |
| 560 | 0.986 | 0.997 | 0.924 | 1.019 | 4.141 | 0.983 | 1.016 | 1.028 | 0.969 | 0.898 | 0.915 | 1.008 |
| 580 | 0.986 | 0.997 | 0.924 | 1.020 | 4.216 | 0.982 | 1.017 | 1.029 | 0.968 | 0.893 | 0.911 | 1.013 |
| 600 | 0.985 | 0.997 | 0.925 | 1.021 | 4.281 | 0.981 | 1.017 | 1.031 | 0.966 | 0.889 | 0.907 | 1.019 |

Westcott *g* Factors Extended to Arbitrary Neutron Energy Spectra

| <i>T</i> (K) | ^{192}Ir | ^{193}Ir | ^{190}Os | ^{196}Hg | ^{199}Hg | ^{197}Au | ^{204}Hg | ^{229}Th | ^{232}Th | ^{231}Pa | ^{233}Pa | ^{234}U |
|--------------|-------------------|-------------------|-------------------|-------------------|-------------------|-------------------|-------------------|-------------------|-------------------|-------------------|-------------------|------------------|
| 20 | 0.865 | 0.973 | 1.023 | 1.023 | 1.021 | 0.992 | 0.415 | 0.957 | 1.011 | 1.199 | 1.107 | 1.019 |
| 40 | 0.885 | 0.978 | 1.019 | 1.019 | 1.017 | 0.994 | 0.552 | 0.964 | 1.009 | 1.161 | 1.088 | 1.016 |
| 60 | 0.906 | 0.982 | 1.015 | 1.016 | 1.014 | 0.995 | 0.652 | 0.970 | 1.007 | 1.127 | 1.071 | 1.013 |
| 80 | 0.928 | 0.986 | 1.012 | 1.012 | 1.011 | 0.996 | 0.735 | 0.977 | 1.006 | 1.099 | 1.055 | 1.010 |
| 100 | 0.952 | 0.990 | 1.008 | 1.009 | 1.008 | 0.997 | 0.807 | 0.984 | 1.004 | 1.075 | 1.040 | 1.007 |
| 120 | 0.978 | 0.994 | 1.005 | 1.005 | 1.004 | 0.999 | 0.871 | 0.992 | 1.002 | 1.054 | 1.027 | 1.004 |
| 140 | 1.006 | 0.999 | 1.001 | 1.001 | 1.001 | 1.000 | 0.931 | 0.999 | 1.001 | 1.037 | 1.014 | 1.001 |
| 160 | 1.037 | 1.003 | 0.998 | 0.998 | 0.998 | 1.001 | 0.985 | 1.007 | 0.999 | 1.022 | 1.002 | 0.998 |
| 180 | 1.071 | 1.007 | 0.995 | 0.994 | 0.995 | 1.002 | 1.037 | 1.015 | 0.998 | 1.009 | 0.991 | 0.995 |
| 200 | 1.109 | 1.012 | 0.991 | 0.991 | 0.992 | 1.004 | 1.085 | 1.024 | 0.996 | 0.999 | 0.981 | 0.992 |
| 220 | 1.152 | 1.017 | 0.988 | 0.988 | 0.989 | 1.005 | 1.131 | 1.033 | 0.994 | 0.991 | 0.971 | 0.990 |
| 240 | 1.200 | 1.021 | 0.984 | 0.984 | 0.986 | 1.006 | 1.175 | 1.042 | 0.993 | 0.985 | 0.962 | 0.987 |
| 260 | 1.256 | 1.026 | 0.981 | 0.981 | 0.983 | 1.008 | 1.217 | 1.051 | 0.991 | 0.982 | 0.954 | 0.984 |
| 280 | 1.319 | 1.031 | 0.978 | 0.977 | 0.979 | 1.009 | 1.257 | 1.061 | 0.990 | 0.980 | 0.946 | 0.981 |
| 293 | 1.364 | 1.034 | 0.976 | 0.975 | 0.978 | 1.010 | 1.282 | 1.067 | 0.989 | 0.980 | 0.941 | 0.980 |
| 300 | 1.389 | 1.035 | 0.975 | 0.974 | 0.976 | 1.010 | 1.295 | 1.071 | 0.988 | 0.981 | 0.939 | 0.979 |
| 320 | 1.469 | 1.040 | 0.971 | 0.971 | 0.973 | 1.012 | 1.333 | 1.081 | 0.987 | 0.984 | 0.932 | 0.976 |
| 340 | 1.556 | 1.045 | 0.968 | 0.968 | 0.971 | 1.013 | 1.369 | 1.092 | 0.985 | 0.991 | 0.925 | 0.973 |
| 360 | 1.652 | 1.050 | 0.965 | 0.964 | 0.968 | 1.014 | 1.404 | 1.104 | 0.984 | 1.001 | 0.919 | 0.971 |
| 380 | 1.756 | 1.055 | 0.962 | 0.961 | 0.965 | 1.016 | 1.437 | 1.116 | 0.982 | 1.015 | 0.914 | 0.968 |
| 400 | 1.867 | 1.061 | 0.959 | 0.958 | 0.962 | 1.017 | 1.470 | 1.128 | 0.980 | 1.034 | 0.908 | 0.965 |
| 420 | 1.984 | 1.066 | 0.955 | 0.955 | 0.959 | 1.018 | 1.502 | 1.142 | 0.979 | 1.058 | 0.903 | 0.963 |
| 440 | 2.107 | 1.071 | 0.952 | 0.952 | 0.956 | 1.020 | 1.533 | 1.156 | 0.977 | 1.089 | 0.899 | 0.960 |
| 460 | 2.234 | 1.077 | 0.949 | 0.948 | 0.953 | 1.021 | 1.564 | 1.172 | 0.976 | 1.128 | 0.894 | 0.958 |
| 480 | 2.365 | 1.082 | 0.946 | 0.945 | 0.950 | 1.022 | 1.594 | 1.189 | 0.974 | 1.173 | 0.890 | 0.955 |
| 500 | 2.500 | 1.088 | 0.943 | 0.942 | 0.947 | 1.024 | 1.623 | 1.209 | 0.973 | 1.228 | 0.886 | 0.953 |
| 520 | 2.636 | 1.093 | 0.940 | 0.939 | 0.945 | 1.025 | 1.651 | 1.230 | 0.971 | 1.291 | 0.883 | 0.950 |
| 540 | 2.774 | 1.099 | 0.937 | 0.936 | 0.942 | 1.026 | 1.679 | 1.254 | 0.970 | 1.363 | 0.879 | 0.948 |
| 560 | 2.912 | 1.105 | 0.934 | 0.933 | 0.939 | 1.028 | 1.706 | 1.281 | 0.968 | 1.444 | 0.876 | 0.945 |
| 580 | 3.051 | 1.111 | 0.931 | 0.930 | 0.936 | 1.029 | 1.733 | 1.313 | 0.967 | 1.536 | 0.873 | 0.943 |
| 600 | 3.189 | 1.117 | 0.928 | 0.927 | 0.934 | 1.030 | 1.759 | 1.348 | 0.966 | 1.636 | 0.871 | 0.940 |

Westcott *g* Factors Extended to Arbitrary Neutron Energy Spectra

| <i>T</i> (K) | ^{235}U | ^{238}U | ^{237}Np | ^{239}Pu | ^{240}Pu | ^{241}Pu | ^{241}Am | ^{242}Am | ^{243}Am | ^{249}Cf | ^{252}Cf | ^{249}Bk |
|--------------|------------------|------------------|-------------------|-------------------|-------------------|-------------------|-------------------|-------------------|-------------------|-------------------|-------------------|-------------------|
| 20 | 1.095 | 0.998 | 1.044 | 0.957 | 0.959 | 1.187 | 1.118 | 0.935 | 0.981 | 1.124 | 1.010 | 0.859 |
| 40 | 1.088 | 0.998 | 1.037 | 0.955 | 0.966 | 1.151 | 1.095 | 0.945 | 0.984 | 1.103 | 1.008 | 0.878 |
| 60 | 1.076 | 0.999 | 1.030 | 0.960 | 0.972 | 1.120 | 1.075 | 0.955 | 0.987 | 1.083 | 1.007 | 0.899 |
| 80 | 1.061 | 0.999 | 1.023 | 0.969 | 0.978 | 1.093 | 1.058 | 0.966 | 0.990 | 1.064 | 1.005 | 0.924 |
| 100 | 1.046 | 0.999 | 1.017 | 0.983 | 0.985 | 1.071 | 1.044 | 0.976 | 0.993 | 1.047 | 1.004 | 0.953 |
| 120 | 1.033 | 1.000 | 1.010 | 0.999 | 0.992 | 1.052 | 1.032 | 0.987 | 0.996 | 1.031 | 1.002 | 0.987 |
| 140 | 1.021 | 1.000 | 1.005 | 1.019 | 0.998 | 1.037 | 1.022 | 0.998 | 0.999 | 1.015 | 1.001 | 1.027 |
| 160 | 1.009 | 1.001 | 0.999 | 1.041 | 1.005 | 1.025 | 1.013 | 1.010 | 1.003 | 1.001 | 0.999 | 1.076 |
| 180 | 0.999 | 1.001 | 0.994 | 1.066 | 1.012 | 1.016 | 1.006 | 1.021 | 1.006 | 0.988 | 0.998 | 1.140 |
| 200 | 0.990 | 1.001 | 0.988 | 1.094 | 1.019 | 1.010 | 1.001 | 1.033 | 1.009 | 0.975 | 0.997 | 1.223 |
| 220 | 0.983 | 1.002 | 0.984 | 1.125 | 1.027 | 1.008 | 0.997 | 1.045 | 1.013 | 0.964 | 0.995 | 1.332 |
| 240 | 0.976 | 1.002 | 0.979 | 1.161 | 1.034 | 1.008 | 0.995 | 1.057 | 1.016 | 0.953 | 0.994 | 1.472 |
| 260 | 0.970 | 1.003 | 0.975 | 1.201 | 1.042 | 1.013 | 0.995 | 1.070 | 1.020 | 0.943 | 0.992 | 1.647 |
| 280 | 0.964 | 1.003 | 0.971 | 1.247 | 1.049 | 1.020 | 0.998 | 1.082 | 1.023 | 0.933 | 0.991 | 1.860 |
| 293 | 0.961 | 1.003 | 0.968 | 1.280 | 1.054 | 1.028 | 1.002 | 1.091 | 1.026 | 0.928 | 0.990 | 2.018 |
| 300 | 0.960 | 1.003 | 0.967 | 1.299 | 1.057 | 1.032 | 1.004 | 1.095 | 1.027 | 0.925 | 0.990 | 2.110 |
| 320 | 0.956 | 1.004 | 0.964 | 1.358 | 1.065 | 1.047 | 1.014 | 1.108 | 1.031 | 0.916 | 0.988 | 2.395 |
| 340 | 0.954 | 1.004 | 0.961 | 1.425 | 1.073 | 1.066 | 1.028 | 1.121 | 1.035 | 0.909 | 0.987 | 2.712 |
| 360 | 0.952 | 1.005 | 0.958 | 1.500 | 1.081 | 1.089 | 1.047 | 1.135 | 1.039 | 0.902 | 0.985 | 3.056 |
| 380 | 0.950 | 1.005 | 0.956 | 1.583 | 1.089 | 1.115 | 1.071 | 1.148 | 1.043 | 0.895 | 0.984 | 3.423 |
| 400 | 0.949 | 1.005 | 0.955 | 1.675 | 1.098 | 1.144 | 1.101 | 1.162 | 1.047 | 0.890 | 0.983 | 3.806 |
| 420 | 0.949 | 1.006 | 0.954 | 1.776 | 1.107 | 1.177 | 1.136 | 1.175 | 1.052 | 0.884 | 0.981 | 4.202 |
| 440 | 0.950 | 1.006 | 0.954 | 1.885 | 1.115 | 1.211 | 1.178 | 1.189 | 1.057 | 0.880 | 0.980 | 4.603 |
| 460 | 0.950 | 1.007 | 0.955 | 2.001 | 1.124 | 1.248 | 1.225 | 1.203 | 1.062 | 0.875 | 0.979 | 5.007 |
| 480 | 0.952 | 1.007 | 0.958 | 2.125 | 1.134 | 1.287 | 1.279 | 1.217 | 1.067 | 0.872 | 0.978 | 5.409 |
| 500 | 0.953 | 1.008 | 0.961 | 2.256 | 1.143 | 1.328 | 1.338 | 1.230 | 1.072 | 0.869 | 0.976 | 5.805 |
| 520 | 0.955 | 1.008 | 0.967 | 2.393 | 1.153 | 1.370 | 1.403 | 1.244 | 1.078 | 0.866 | 0.975 | 6.193 |
| 540 | 0.958 | 1.008 | 0.974 | 2.535 | 1.163 | 1.412 | 1.473 | 1.258 | 1.084 | 0.864 | 0.974 | 6.569 |
| 560 | 0.960 | 1.009 | 0.983 | 2.681 | 1.173 | 1.455 | 1.547 | 1.271 | 1.090 | 0.863 | 0.973 | 6.933 |
| 580 | 0.963 | 1.009 | 0.995 | 2.831 | 1.183 | 1.498 | 1.626 | 1.285 | 1.096 | 0.862 | 0.971 | 7.281 |
| 600 | 0.966 | 1.010 | 1.008 | 2.984 | 1.194 | 1.542 | 1.709 | 1.298 | 1.103 | 0.862 | 0.970 | 7.613 |